Inflammation (© 2016)
DOI: 10.1007/s10753-016-0371-x

ORIGINAL ARTICLE

Effect of Low-Power Laser (LPL) and Light-Emitting Diode (LED) on Inflammatory Response in Burn Wound Healing

Paulo C. L. Silveira,[1,2] Karina B. Ferreira,[1] Franciani R. da Rocha,[1] Bruno L. S. Pieri,[1] Giulia S. Pedroso,[1] Claudio T. De Souza,[1] Renata T. Nesi,[1] and Ricardo A. Pinho[1]

Abstract—The aim of the study was to investigate the biochemical and molecular changes in the process of epidermal healing of burn injuries after therapeutic treatment with low-power laser (LPL) and light-emitting diode (LED). Rats were divided into six groups: skin without injury (Sham), burn wounds (BWs), BW + 660-nm LPL, BW + 904-nm LPL, BW + 632-nm LED, and BW + 850-nm LED. The burn wound model was performed using a 100 °C copper plate, with 10 s of contact in the skin. The irradiations started 24 h after the lesion and were performed daily for 7 days. The burn wound groups showed an increase in the superoxide production, dichlorofluorescein, nitrites, and high protein oxidative damage. The activities of glutathione peroxidase and catalase were also increased, and a significant reduction in glutathione levels was observed compared to the control group. However, treatments with 660-nm LPL and 850-nm LED promoted protection against to oxidative stress, and similar results were also observed in the IL-6 and pERK1/2 expression. Taken together, these results suggest that LPL 660 nm and LED 850 nm appear reduced in the inflammatory response and oxidative stress parameters, thus decreasing dermal necrosis and increasing granulation tissue formation, in fact accelerating the repair of burn wounds.

KEY WORDS: dermal burn lesion; inflammation; LED; low-power laser; oxidative stress.

INTRODUCTION

Tissue damage triggers a cascade of biochemical and molecular events that initiate a rapid but highly complex tissue repair process [1]. Wound healing is one of the most complex biological events and results from the interactions between different tissue structures and a large number of infiltrative cells, including mainly neutrophils, macrophages, mast cells, and lymphocytes, which serve as immune effector cells as well as a source of cytokines and growth factors [2].

The process of wound healing comprises a series of events characterized by distinct but overlapping stages, namely inflammation, epithelialization, connective tissue deposition, and contraction, which all involve the actions of specific cells and numerous cytokines [3, 4]. Although burns have traditionally been regarded as a special type of wound that requires specialized treatment protocols, in many ways, healing of burn wounds is no different from any other form of healing, which occurs independently of the origin of the lesion [3].

Reactive oxygen species (ROS) and reactive nitrogen species (RNS) contribute to increased tissue damage in events such as burn wounds and are known to impair the healing process [5]. During the healing process, ROS and RNS play a crucial role in wound healing, particularly in the inflammatory phase [6]. Moreover, the activated

[1] Laboratory of Biochemistry of Exercise and Physiology, PPGCS, Post-Graduate Program in Health Sciences, Health Sciences Unit, Av. Universitária, 1105 Universitário–Block S, room 16, Zip Code 88806-000 Criciúma, SC, Brazil

[2] To whom correspondence should be addressed at Laboratory of Biochemistry of Exercise and Physiology, PPGCS, Post-Graduate Program in Health Sciences, Health Sciences Unit, Av. Universitária, 1105 Universitário–Block S, room 16, Zip Code 88806-000 Criciúma, SC, Brazil. E-mail: psilveira@unesc.net

Published online: 20 May 2016

neutrophils activate the nicotinamide adenine dinucleotide phosphate-oxidase complex, which can produce excess superoxide, thereby altering the cellular redox state and delaying the process of tissue repair [7]. Based on the above considerations, substances or therapies that stimulate the repair ability and antioxidant defense are important to maintain low levels of free radical production and allow the recovery of skin burns [8].

Several studies have reported the development of increasingly efficient approaches for tissue repair, with minimization of the factors that delay or impede the healing process [9]. Among the current approaches, the use of low-power laser (LPL) and light-emitting diode (LED) has shown good results and has attracted the attention of the scientific community [10, 11].

The use of LED and LPL has proven effective in controlling pain and reducing the healing time by stimulating collagen production, fibroblast proliferation, and the local microvasculature [7, 12–15], as well as by stimulating cellular metabolism and increasing the potential for tissue regeneration [16, 17]. On the other hand, the effects of LED and LPL on the levels of ROS generated by tissue lesions are currently unknown. However, the reduction of ROS appears to be involved in the anti-inflammatory effects of LPL and LED, which have been shown to reduce the activation of various transcription factors and pro-inflammatory interleukins (ILs) [18, 19]. Thus, from these assumptions, this study aimed to investigate the changes in oxidative stress parameters and inflammatory mediators during the healing of epidermal damage induced by burns after therapeutic treatment with LPL and LED.

METHODS

Animals

Fifty male Wistar rats (250–300 g) were obtained from the breeding colony of Universidade do Extremo Sul Catarinense (protocol committee of ethics—69/2014-1). Animals were kept in cages in a room temperature at 23 ± 1 °C with ad libitum access to water and food under 12-h dark/light cycles. Animals were divided into six groups ($N = 10$): skin without injury (Sham), burn wounds (BWs), BW + LPL 660 nm, BW + LPL 904 nm, BW + LED 632 nm, and BW + LED 850 nm.

Skin Injury Protocol

Animals were anesthetized with an intraperitoneal injection of ketamine (80 mg/kg) and xylazine (20 mg/kg). Then, the dorsal region was shaved. The second-degree burn model was induced using a 20 × 10 × 10-mm copper plate at 100 °C for 10 s according to Xiao *et al*. [20]. Rats were given dipyrone (80 mg/kg), and the control animals underwent anesthetic protocol.

Irradiation Protocol

The LPL was used in this study with GaAs pulsed emission (wavelength 904 nm; 70-W peak power, frequency 9500 Hz, pulse time of 60 ns; 0.10-cm^2 beam size, power density of 0.4/cm^2, dose 3 J/cm^2, and time of irradiation 9 s), the AlGaInP laser with continuous emission (wavelength 660 nm, 30-mW peak power; 0.10-cm^2 beam size, dose 10 J/cm^2, and time of irradiation 20 s), and the two lasers from Laser Pulse-Ibramed company (Sao Paulo, Brazil). Irradiation was performed in five distinct regions around the wound as previously described by Prado [21]. The red LED (wavelength 632 nm, intensity of 100 %, frequency 80 Hz, duty cycle 20 %, effective radiation area of 160 cm^2, optical power density of 14 mW/cm^2, 402 emitter points, and 10-min application time) and infrared (850-nm wavelength intensity of 100 %, frequency 80 Hz, duty cycle 20 %, effective radiation area of 160 cm^2, optical power density of 33 mW/cm^2, emitting points 402, and 10-min application time) were used. The animals were irradiated by seven sessions, one time per day, and 24 h after the induction of the burn.

Euthanasia and Sample Preparation

Two hours after the last irradiation session, the animals were sacrificed by decapitation and the external border of the injured region was removed. The tissue was homogenized in the specific buffer and centrifuged at 1.000×*g* for 10 min at 4 °C, and the supernatants were kept at −70°C until analysis.

Macroscopic Evaluation of Wound Contraction

Before euthanization, the wounds were photographed using a tripod from a standard distance of 25 cm. The surface area of wounds was calculated and compared with "ImageJ" computer program from the photographs.

Histology

Immediately after euthanasia, the tissue was embedded in 10 % paraformaldehyde followed by successive alcohol and xylol baths, embedded in paraffin, and cut into 5-mm-thick slices. Tissue slices were fixed and stained with hematoxylin and eosin (H&E) and analyzed by light microscopy for analysis of cellular necrosis, vascular

occlusion, the granulation tissue, and the effect of the burn in the normal layers (dermis, epidermis, and hypodermis) of the skin [22].

Biochemical Assays

Protein Analysis by Western Blot

Proteins were denatured by boiling in sample buffer containing 100 mM DTT [23]. After this, 0.2 mg of protein extracts was separated by SDS-PAGE, transferred to nitrocellulose membranes, and blotted with anti-extracellular signal-regulated kinase (ERK) 1/2 phosphorylation or anti-interleukin 6 or IL6 (Santa Cruz Biotechnology, Santa Cruz, CA, USA). Chemiluminescent detection was performed using horseradish peroxidase-conjugated secondary antibodies. Visualization of protein bands was performed by exposure of the membranes to RX films. The original membrane was stripped and reblotted with actin loading protein. After transfer, the membrane was stained with Ponceau and the bands were visualized, photographed, and quantified before the primary antibody, to control the transfer. Band intensities were quantitated by optical densitometry (Scion Image Software, ScionCorp, Frederick, MD, USA) of the developed autoradiographs. Beta actin antibody (Abcam) was used as a loading control for Western blot analysis.

Determination of Intracellular ROS and Nitric Oxide

Anion superoxide was determined from submitochondrial particles (SMP), and the level of superoxide was estimated by measuring adrenaline oxidation spectrophotometrically at 780 nm [24]. The intracellular 2′,7′-dichlorofluorescein (DCF) oxidized levels were monitored from samples incubated with DCFH-DA. The formation of the oxidized fluorescent derivate was monitored at excitation and emission wavelengths of 488 and 525 nm, respectively, using a fluorescence spectrophotometer [25]. Nitric oxide was estimated spectrophotometrically from nitrite generation. The samples were incubated with Griess reagent at room temperature, and the absorbance was measured at 540 nm using a microplate reader [26].

Oxidative Damage

Protein carbonyl content was measured by labeled protein hydrazone derivatives using 2,4-dinitrophenylhydrazide. These derivatives were extracted with trichloroacetic acid followed by treatment with ethanol/ethyl acetate and dissolved in urea hydrochloride. The concentration of 2.4-dinitrophenylhydrazide incorporated was expressed per milligram of protein at 370 nm [27]. The total thiol content was determined using the 5,5′-dithiobis(2-nitrobenzoic acid), and the absorbance was measured at 412 nm using a spectrophotometer [28].

Antioxidant System

Catalase activity was measured using the rate of decrease in hydrogen peroxide absorbance at 240 nm [29]. Glutathione peroxidase activity was measured by monitoring the oxidation of NADPH at 340 nm in the presence of tert-butylhydroperoxide [30]. Total glutathione levels were determined in tissue homogenates in the presence of DTNB. Color development resulting from the reaction was expressed per milligram of protein at 412 nm [31].

Protein Content

Protein content from tissue was assayed using bovine serum albumin as a standard, according to Lowry and colleagues [32].

Statistical Analysis

Differences among the experimental groups are presented as mean ± SEM. Differences among groups were determined by one-way ANOVA, followed by Tukey's post hoc test when ANOVA was significant; p values less than 0.05 were considered statistically significant. The software used for data analysis was the Statistical Package for the Social Sciences (SPSS) version 18.0 for Microsoft Windows.

RESULTS

Healing

Figure 1 shows the effect of applying LPL and LED on the quantification of wound contraction. Significant improvements in the wound healing, as measured by the reduction in wound size, could be observed in animals irradiated with 660-nm LPL and 850-nm LED compared to the lesion group.

Histology

Figure 2 shows the effect of LPL and LED treatment on the skin tissue after burn model. Figure 2a shows the histological appearance in the control group with all the layers of the skin, including the glandular structures,

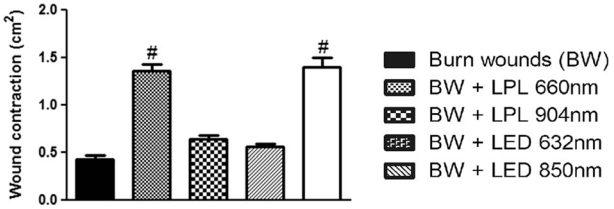

Fig. 1. Macroscopic effects were measured through the reduction of the wound area 7 days after the burn model daily treated by applications of LED and LPL.

numerous hair follicles (black star), and well-developed dermal papillae, while the burned skin (Fig. 2b) presented diffuse epidermal and dermal necrosis (black star). Animals that were burned developed a superficial second-degree burn (damage limited to the upper third of the dermis). The burned skin treated by laser 660-nm group (Fig. 2c) presented well-developed dermal papillae (black star), while the laser 904-nm treatment (Fig. 2d) still presented higher evidence of dermal necrosis (black star), in turn, both laser 660- and 904-nm groups compared to the burned group. On the other hand, the burned skin treated with LED 630 (Fig. 2e) and 850 (Fig. 2f) demonstrated a better organization of the tissue, similar to the control group, showing granulation tissue below the epidermis layer (black star) when compared to the burned group, showing a similar pattern of granulation tissue, hair follicles, and well-developed dermal papillae.

Levels of IL-6 and ERK1/2

Figure 3a, b depicts the levels of ERK1/2 phosphorylation and IL-6, respectively. As for the phosphorylation of ERK1/2, a statistically significant decrease was observed in the lesion group compared with the control group. However, the 660-nm laser and 850-nm LED groups conversely showed statistically significant increases when compared to the control group and the lesion group. In the analysis of IL-6, statistically significant increases were observed in the lesion, 904-nm laser, and 660-nm LED groups compared to the control group. Furthermore, the 660-nm laser and 850-nm LED groups showed statistically significant decreases compared to the lesion group ($P < 0.01$).

Oxidant Production

The levels of superoxide, levels of nitrite, and oxidation of 2′-7′-dichlorodihydrofluorescein diacetate were investigated as oxidative parameters (Fig. 4a–c, respectively). As seen in Fig. 4a, we observed a statistically significant increase in the lesion, 904-nm laser, and 632-nm LED

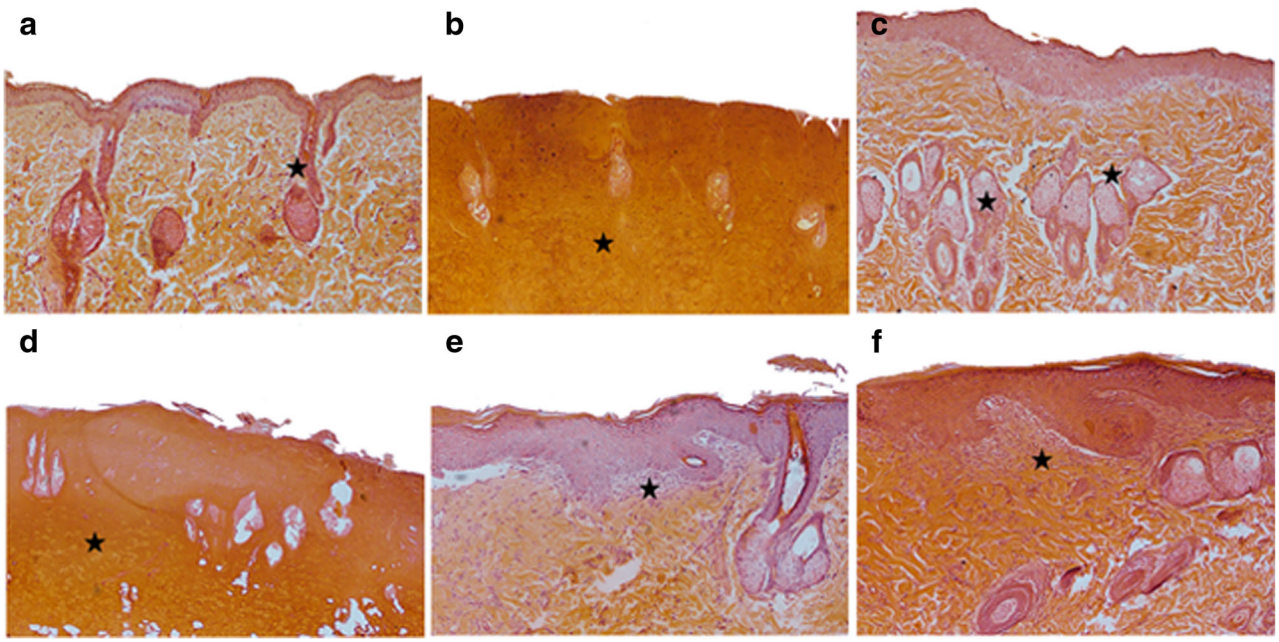

Fig. 2. Photomicrographs of the skin after burn model (**a**–**f**) showing control group (**a**), burned group (**b**), and the following treatment groups with different specificities of LED and LPL applications. Treating the burn lesions with LPL 660-nm laser (**c**) and 904-nm laser (**d**) or using the LED with 632 nm (**e**) and 850 nm (**f**) showing the histopathological profile of the burned tissue after the treatments, ×10 H&E ($n = 3$ per group). The *black stars* are showing the details regarding granulation tissue and dermal area.

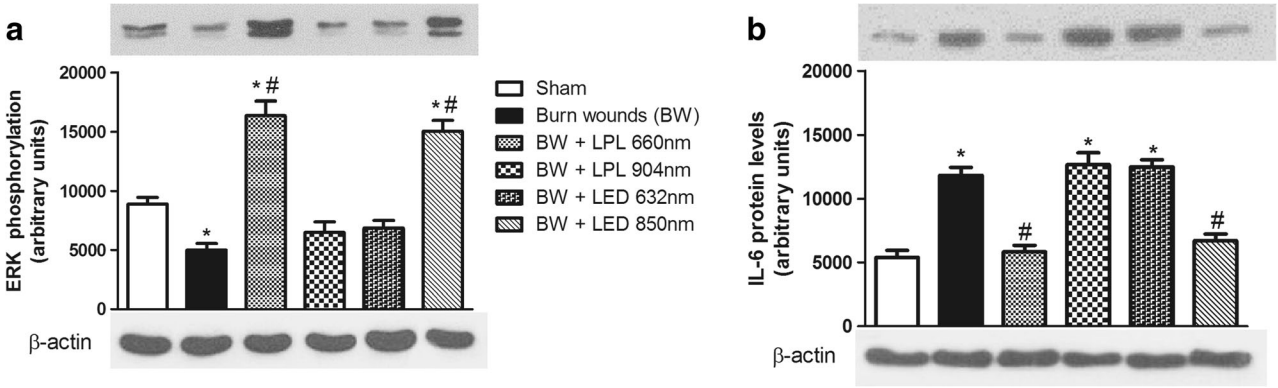

Fig. 3. The inflammatory profile, through the phosphorylated extracellular signal-regulated kinase (p-ERK) (**a**) and interleukin-6 (IL-6) (**b**) content in the skin tissue after burn model. The effects of the LPL and LED daily irradiation in the protein content of **a** ERK and **b** IL-6, after 7 days of the burn model with daily application of LED and LPL. The *bars* represent the mean ± standard error of the mean for seven animals. *$P < 0.01$ vs. control group, #$P < 0.01$ vs. lesion group (one-way ANOVA followed by Tukey's post hoc test).

groups when compared to the control group. However, in the groups treated with the 660-nm laser and 850-nm LED, statistically significant reductions were observed compared with the lesion group. Regarding the levels of dichlorofluorescein (Fig. 4b), the lesion group showed a significant increase compared to the control group; however, the other groups showed significant reductions compared with the lesion group. As seen in Fig. 4c, the lesion and 904-nm laser groups showed significant increases in the levels of nitrite compared to the control group, whereas

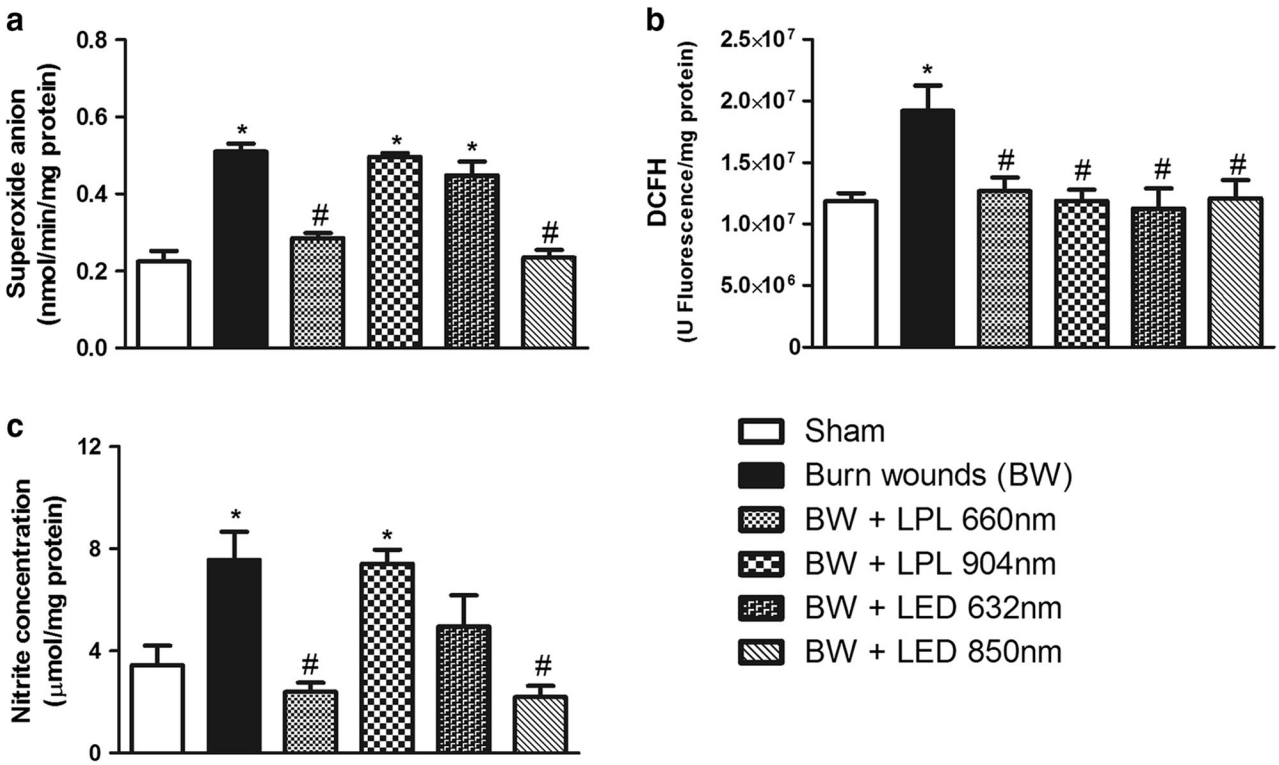

Fig. 4. The oxidant production in the skin tissue after 7 days of the burned model with daily irradiation of LPL and LED. The following biomarkers, superoxide (**a**), the content of 2′-7′-dichlorodihydrofluorescein diacetate (**b**), and nitrite (**c**), were analyzed 7 days after the burn model and treatment were established. The *bars* represent the mean ± standard error of the mean for seven animals. *$P < 0.01$ vs. control group, #$P < 0.01$ vs. lesion group (one-way ANOVA followed by Tukey's post hoc test).

the 660-nm laser and 850-nm LED groups showed significant reductions compared to the lesion group.

Oxidative Damage

Oxidative damage was analyzed according to the levels of protein carboxylation and oxidation of thiol groups. As shown in Fig. 5a, there was a statistically significant increase in the levels of carbonyl in the lesion, 904-nm laser, and 632-nm LED groups compared to the control group. In addition, the 660-nm laser and 850-nm LED groups were found to induce significant decreases relative to the lesion group. In terms of the oxidation of thiol (Fig. 5b), a statistically significant reduction was observed in the lesion group compared to the control. However, the groups treated with 632-nm LED and 850-nm laser showed statistically significant increases in the total thiols when compared to the lesion group ($P < 0.01$).

Antioxidant System

Catalase (Fig. 5c), glutathione peroxidase (Fig. 5d), and total glutathione levels (Fig. 5e) were measured as parameters of the antioxidant system. The glutathione peroxidase activity in the lesion group was found to be statistically increased compared to the control group; however, the 660-nm laser and 850-nm LED groups displayed significant reductions compared with the lesion group. Regarding the activity of catalase, the lesion group also showed a significant increase compared to the control groups, whereas the groups receiving 660-nm laser, 632-nm LED, and 830-nm LED all demonstrated significant decreases compared to the lesion group. In terms of the total plasma glutathione, the lesion and 632-nm LED groups induced significant increases compared to the control group, whereas the 660-nm laser and 850-nm LED groups showed significantly increased glutathione levels compared to the lesion group.

DISCUSSION

In this study, we used an experimental rat model of epithelial burn injury to evaluate the influence of LPL and LED on wound size and inflammatory and oxidative stress parameters involved in tissue healing. To evaluate wound contraction, we measured the size of the edges as a reference and calculated the total area of the wound in square centimeter using the software ImageJ. As seen in Fig. 1, greater decreases in wound closure were observed in the 660-nm laser and 850-nm LED groups compared to the lesion group. This suggested that these treatments were indeed effective, and we hence further investigated the mechanisms involved in this process of reduction and acceleration of wound healing by analyzing the effects on inflammatory parameters and oxidative stress markers.

The inflammatory response induced by burning wounds is characterized by infiltration of neutrophils in the first 24 h and by subsequent accumulation of macrophages and other immune cells in the injured tissue [33]. Neutrophils and monocytes play key roles in the inflammatory phase of wound repair as they secrete pro-inflammatory cytokines and growth factors [34, 35]. However, these events also increase the production of oxidants, which in turn leads to oxidative damage to lipids, proteins, and DNA, as well as cellular necrosis, thus impairing the recovery of the tissue [36]. Therefore, the enhanced reduction in the size of the wounds observed here suggests a bio-stimulatory effect on the healing process induced by the 660-nm laser and 850-nm LED. Probably, this effect may be related to the optical power density of these two groups, which is roughly equal. Several studies argue that depending on the optical power biostimulatorious, the effects are different for each type of irradiated tissue [37–39]. According to this hypothesis, the histological appearance also showed different effects between the treatments. The burned skin treated by 660-nm laser demonstrated well-developed dermal papillae and also decreased the dermal necrosis area, while the 904-nm laser did not affect the tissue maintaining the dermal necrosis. In turn, in the laser treatment, only the 660 nm appears to be effective to the wound healing in the burned skin. On the other hand, the LED treatment showed both, with the 630 and 850 nm, a better organization of the tissue, showing a higher area of granulation tissue right below the epidermis layer, the presence of hair follicles, and well-developed dermal papillae as the control.

In this scenario, the beneficial effects of LPL and LED may be related to the acceleration of the inflammatory phase and decrease of their harmful effects. Our group has previously demonstrated that the inflammatory phase is accelerated by LPL as a result of increased production of mitochondrial ATP [7, 17, 40, 41]. Moreover, biostimulator effects of LPL have been observed on a variety of mitochondrial enzymes (complexes of proteins in the electron transport chain) in several previous studies [42, 43].

To better understand the effects of LPL and LED on the stimulation of the inflammatory processes, we next

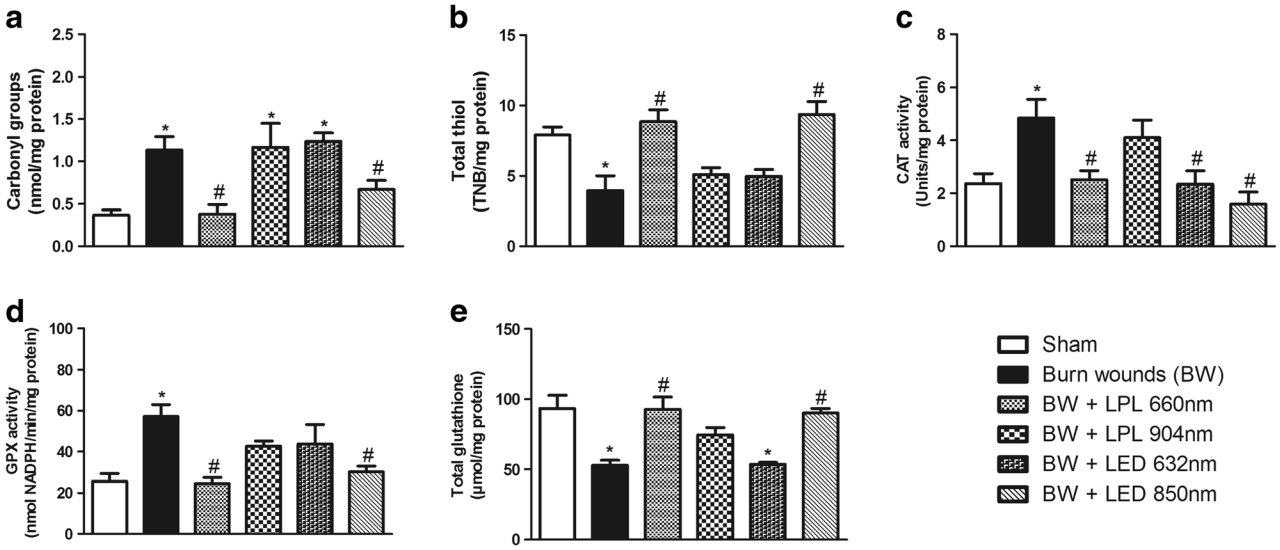

Fig. 5. The oxidative damage and the antioxidant defense after 7 days of the burned model with daily irradiation of LPL and LED. The carbonyl groups (**a**), total thiol content (**b**), catalase (CAT) (**c**), peroxidase glutathione activity (GPx) (**d**), and the content of total glutathione (**e**) were measured 7 days after the burn model was established. The *bars* represent the mean ± standard error of the mean for seven animals. *$P < 0.01$ vs. control group, #$P < 0.01$ vs. lesion group (one-way ANOVA followed by Tukey's post hoc test).

evaluated the phosphorylation of ERK1/2 (Fig. 3a, b), which belongs to the mitogen-activated protein kinase (MAPK) cascade and acts inside the cell to induce mitosis and cell division, thereby initiating signaling cascades related to the healing process [44]. As seen in Fig. 3a, the lesion group demonstrated a significant decrease in the levels of ERK1/2, 7 days after the BW model was created, suggesting that the inflammatory response may still have been in the acute phase, which is characterized by an absence of cell proliferation and differentiation. However, the 660-nm laser and 850-nm LED groups showed significant increases of these proteins relative to the lesion group, likely owing to the inflammatory process being at a more advanced stage, thus resulting in the release of growth factors and increased phosphorylation and activation of the MAPK pathway.

To confirm the inflammatory response, we measured the content of IL-6, as damage to the skin, such as burns, is known to cause inflammation by stimulating cytokine production (including IL-6 production) by keratinocytes [45]. After acute rupture of the epidermal barrier, there is an increase in the expression of IL-1, tumor necrosis factor alpha (TNF-α), and IL-6, which are all potent stimulators of epithelial, mitogenic, and lipid synthesis [46]. These cytokines appear to be essential for the repair of the skin barrier. However, if the rupture of the barrier is extended with a chronic increase in cytokine production, detrimental effects on inflammation and epidermal proliferation may occur [47]. As shown in Fig. 3b, the lesion group exhibited a significant increase in the IL-6 levels 7 days after the burn compared to the control group, suggesting a delay in epithelial wound healing. Meanwhile, the 660-nm laser and 850-nm LED groups demonstrated decreases in the IL-6 levels compared to the lesion group, confirming the results observed for ERK1/2, which demonstrated an improvement in the inflammatory response induced by the LED and LPL.

In addition, some authors have suggested that the observed effects may be due to decreased production of SRN and ROS induced by LPL and LED, which, in high concentrations, can lead to amplification of the inflammatory response by stimulating a large release of pro-inflammatory cytokines such as IL-1β, TNF-α, and IL-6 [48–51]. There is evidence in the literature that LED and LPL reduce the production of reactive oxygen and nitrogen species that occur during the acute phase of muscle and epithelial lesions. Previous studies [40, 41, 52–54] showed that infrared irradiation decreased the synthesis of peroxynitrite via dissociation of superoxide and nitric oxide, leading to reduction of oxidative stress and inhibition of the apoptotic pathway in isolated mitochondria. Other previous studies have suggested that the absorption of light can shift the nitric oxide linked to cytochrome c oxidase, thereby recovering in cellular respiration [55], and this mechanism may explain the decrease in oxidative stress observed in our study, with the damaged cells potentially

responding better to the LPL and LED than healthy cells due to cytochrome c oxidase working at a submaximal level as a result of inhibition by nitric oxide [56, 57]. Additionally, two other potential mechanisms have been cited as responsible for this redox modulation, including (I) reduction of the migration and activity of inflammatory cells and a subsequent decline in the production of ROS and RNA and (ii) stimulation of the synthesis or activity of antioxidant enzymes [48, 58]. Furthermore, it is believed that LED and LPL can decrease the activation of nuclear transcription factor kappa β and thus decrease the subsequent transcription of pro-inflammatory cytokines [18, 19]. These molecular mechanisms diminish the capillary hydrostatic pressure, which in turn results in edema absorption induced by the burns and eliminates the chemical mediators of inflammation [59].

The presence of ROS-mediated lipid peroxidation, protein oxidation, and oxidative damage in nucleic acids is considered a crucial event in the cytotoxic action of ROS and ERN. The thiol groups and proteins present on the cell structure are common targets of peroxidative attacks, leading to changes in membrane fluidity and permeability [60]. Our results revealed that the lesion group showed significant increases in these markers, whereas these effects were reversed by the 660-nm laser and 850-nm LED treatments. These decreases in the markers of oxidative damage likely reflect the decreased production of ROS induced by these therapies, as seen in Fig. 4, as well as an improved antioxidant profile of the tissue with the application of both therapies, as discussed below.

As seen in Fig. 5, the lesion group showed significant increases in glutathione peroxidase and catalase activities and a concomitant decrease in the total glutathione levels. However, the groups that received 660-nm laser and 850-nm LED treatments showed reversal of these effects in all parameters. It is possible that biochemical modulation occurs due to a decrease in the inflammatory response and, consequently, a reduction in ROS. Glutathione peroxidase and catalase play important roles in the defense against oxidative stress and are inducible because their activities depend on the concentration of peroxide. The decreased activity of glutathione peroxidase and catalase from the treatment (LPL and LED) may be an indicative of a reduction of oxidative stress in the epithelial tissue [61]. In addition, the glutathione is one of the most important non-enzymatic antioxidants in epithelial tissue and functions mainly by reacting with a variety of free radicals by donating a hydrogen atom and/or by serving as a substrate for glutathione peroxidase to eliminate hydrogen peroxide and organic hydroperoxides, as well as being involved in the reduction of other antioxidants [62]. Thus, the reduction in the levels of total glutathione observed after BWs is likely associated with excessive production of ROS and a reduced ability of the skin to resynthesize glutathione under these conditions [63].

Taken together, the data presented in this study indicate that the use of LPL and LED can reduce the inflammatory response induced by our experimental BW model, likely by blocking the effects of ROS via activation of IL-6 and inhibition of cell proliferation and differentiation induced by growth factors via the MAPK pathway. These results can help explain the therapeutic potential of LPL and LED in reducing the negative consequences of inflammation by optimizing epithelial healing. However, further studies using these therapies are needed to elucidate the exact mechanisms involved in the epithelial inflammatory BW response.

ACKNOWLEDGMENTS

This research was supported by grants from UNESC, CNPq, and FAPESC.

REFERENCES

1. Martin, P., and S.J. Leibovich. 2005. Inflammatory cells during wound repair: the good, the bad and the ugly. *Trends Cell Biol* 15: 599–607.
2. Gillitzer, R., and M. Goebeler. 2001. Chemokines in cutaneous wound healing. *J Leukoc Biol* 69: 513–521.
3. Atiyeh, B.S., S.W. Gunn, and S.N. Hayek. 2005. State of the art in burn treatment. *World J Surg* 29: 131–148.
4. Diegelmann, R.F., and M.C. Evans. 2004. Wound healing: an overview of acute, fibrotic and delayed healing. *Front Biosci* 1: 9283–9289.
5. Phan, T.T., L. Wang, P. See, R.J. Grayer, S.Y. Chan, and S.T. Lee. 2001. Phenolic compounds of Chromolaena odorata protect cultured skin cells from oxidative damage: implication for cutaneous wound healing. *Biol Pharm Bull* 24: 1373–1379.
6. Serarslan, G., E. Altug, T. Kontas, E. Atik, and G. Avci. 2007. Caffeic acid phenethyl ester accelerates cutaneous wound healing in a rat model and decreases oxidative stress. *Clin Exp Dermatol* 32: 709–715.
7. Silveira, P.C.L., E.L. Streck, and R.A. Pinho. 2007. Evaluation of mitochondrial respiratory chain activity in wound healing by low-level laser therapy. *J Photochem Photobiol B Biol* 8: 6279–6282.
8. Pileggi, C., A. Bianco, D. Flotta, C.G.A. Nobile, and M. Pavia. 2011. Prevention of ventilator-associated pneumonia, mortality and all intensive care unit acquired infections by topically applied antimicrobial or antiseptic agents: a meta-analysis of randomized controlled trials in intensive care units. *Crit Care* 15: 155.
9. Guo, S., and L.A. Dipietro. 2010. Factors affecting wound healing. *J Dent Res* 89: 219–229.

10. Moura Junior, M.J., E.A.L. Arisawa, A.A. Martin, J.P. de Carvalho, J.M.N. da Silva, J.F. Silva, *et al*. 2014. Effects of low-power LED and therapeutic ultrasound in the tissue healing and inflammation in a tendinitis experimental model in rats. *Lasers Med Sci* 29: 301–311.
11. Casalechi, H.L., R.A. Nicolau, V.L. Casalechi, L.J. Silveira, A.M.B. De Paula, and M.T.T. Pacheco. 2009. The effects of low-level light emitting diode on the repair process of Achilles tendon therapy in rats. *Lasers Med Sci* 24: 659–665.
12. Conlan, M.J., J.W. Rapley, and C.M. Cobb. 1996. Biostimulation of wound healing by low-energy laser irradiation. A review. *J Clin Periodontol* 23: 492–496.
13. do Nascimento, P.M., A.L.B. Pinheiro, M.A.C. Salgado, and L.M.P. Ramalho. 2004. A preliminary report on the effect of laser therapy on the healing of cutaneous surgical wounds as a consequence of an inversely proportional relationship between wavelength and intensity: histological study in rats. *Photomed Laser Surg* 22: 513–518.
14. Person, M.D., D.E. Mason, D.C. Liebler, T.J. Monks, and S.S. Lau. 2005. Alkylation of cytochrome c by (glutathion-S-yl)-1,4-benzoquinone and iodoacetamide demonstrates compound-dependent site specificity. *Chem Res Toxicol* 18: 41–50.
15. Pinheiro, A.L.B., G.C.S. Meireles, A.L.B. de Barros Vieira, D. Almeida, C.M. Carvalho, and J.N. dos Santos. 2004. Phototherapy improves healing of cutaneous wounds in nourished and undernourished Wistar rats. *Braz Dent J* 15: I21–8.
16. Karu, T., L. Pyatibrat, and G. Kalendo. 1995. Irradiation with He-Ne laser increases ATP level in cells cultivated *in vitro*. *J Photochem Photobiol B* 27: 219–223.
17. Silveira, P.C.L., L.A. da Silva, D.B. Fraga, T.P. Freitas, E.L. Streck, and R. Pinho. 2009. Evaluation of mitochondrial respiratory chain activity in muscle healing by low-level laser therapy. *J Photochem Photobiol B* 95: 89–92.
18. Pires, D., M. Xavier, T. Araújo, J.A. Silva, F. Aimbire, and R. Albertini. 2011. Low-level laser therapy (LPLT; 780 nm) acts differently on mRNA expression of anti-and pro-inflammatory mediators in an experimental model of collagenase-induced tendinitis in rat. *Lasers Med Sci* 26: 85–94.
19. Basso, F.G., T.N. Pansani, A.P.S. Turrioni, V.S. Bagnato, J. Hebling, and C.A.C. Costa. 2012. *In vitro* wound healing improvement by low-level laser therapy application in cultured gingival fibroblasts. *Int J Dent* 2012: 719452.
20. Xiao, M., L. Li, C. Li, P. Zhang, Q. Hu, L. Ma, *et al*. 2014. Role of autophagy and apoptosis in wound tissue of deep second-degree burn in rats. *Acad Emerg Med* 21: 383–391.
21. Prado, R.P., C.E. Pinfildi, R.E. Liebano, B.S. Hochman, and L.M. Ferreira. 2009. Effect of application site of low-level laser therapy in random cutaneous flap viability in rats. *Photomed Laser Surg* 27: 411–416.
22. Valenca, S.S., and L.C. Porto. 2008. Immunohistochemical study of lung remodeling in mice exposed to cigarette smoke. *J Bras Pneumol* 34: 787–795.
23. Laemmli, U.K. 1970. Cleavage of structural proteins during the assembly of the head of bacteriophage. *Nature* 227: 680–685.
24. Poderoso, J.J., M.C. Carreras, C. Lisdero, N. Riobo, F. Schopfer, and A. Boveris. 1996. Nitric oxide inhibits electron transfer and increases superoxide radical production in rat heart mitochondria and submitochondrial particles. *Arch Biochem Biophys* 328: 85–92.
25. Dong, J., K.K. Sulik, and S. Chen. 2010. The role of NOX enzymes in ethanol-induced oxidative stress and apoptosis in mouse embryos. *Toxicol Let* 193: 94–100.
26. Chae, S.Y., M. Lee, S.W. Kim, and Y.H. Bae. 2004. Protection of insulin secreting cells from nitric oxide induced cellular damage by crosslinked hemoglobin. *Biomaterials* 25: 843–850.
27. Levine, R.L., D. Garland, C.N. Oliver, A. Amici, I. Climent, A.G. Lenz, *et al*. 1990. Determination of carbonyl content in oxidatively modified proteins. *Methods Enzymol* 186: 464–478.
28. Aksenov, M.Y., and W.R. Markesbery. 2001. Changes in thiol content and expression of glutathione redox system genes in the hippocampus and cerebellum in Alzheimer's disease. *Neurosci Lett* 302: 141–145.
29. Aebi, H. 1984. Catalase *in vitro*. *Methods Enzymol* 105: 121–126.
30. Flohe, L., and W.A. Gunzler. 1984. Assays of glutathione peroxidase. *Methods Enzymol* 105: 114–121.
31. Hissin, P.J., and R. Hilf. 1976. A fluorometric method for determination of oxidized and reduced glutathione in tissues. *Anal Biochem* 74: 214–226.
32. Lowry, O.H., N.J. Rosebrough, A.L. Farr, and R.J. Randall. 1951. Protein measurement with the Folin phenol reagent. *J Biol Chem* 193: 265–275.
33. Li, G., X. Feng, and S. Wang. 2005. Effects of Cu/Zn superoxide dismutase on strain injury-induced oxidative damage to skeletal muscle in rats. *Physiol Res* 54: 193–199.
34. Henry, G., and W.L. Garner. 2003. Inflammatory mediators in wound healing. *Surg Clin North Am* 83: 483–507.
35. Pereira, L.M., E. Hatanaka, E.F. Martins, F. Oliveira, E.A. Liberti, S.H. Farsky, *et al*. 2008. Effect of oleic and linoleic acids on the inflammatory phase of wound healing in rats. *Cell Biochem Funct* 26: 197–204.
36. Pattwell, D.M., and M.J. Jackson. 2004. Contraction-induced oxidants as mediators of adaptation and damage in skeletal muscle. *Exerc Sport Sci Ver* 32: 14–18.
37. Gonçalves, R.V., R.D. Novaes, M.C. Cupertino, B. Moraes, J.P.V. Leite, P.M.C. Gouveia, *et al*. 2013. Time-dependent effects of low-level laser therapy on the morphology and oxidative response in the skin wound healing in rats. *Lasers Med Sci* 28: 383–390.
38. Crisan, B., O. Soritau, M. Baciut, R. Campian, L. Crisan, and G. Baciut. 2013. Influence of three laser wavelengths on human fibroblasts cell culture. *Lasers Med Sci* 28: 457–463.
39. Peplow, P.V., T.Y. Chung, B. Ryan, and G.D. Baxter. 2011. Laser photobiomodulation of gene expression and release of growth factors and cytokines from cells in culture: a review of human and animal studies. *Photomed Laser Surg* 29: 285–304.
40. Silveira, P.C.L., L.A. Silva, T.P. Freitas, A. Latini, and R.A. Pinho. 2011. Effects of low-power laser irradiation (LPLI) at different wavelengths and doses on oxidative stress and fibrogenesis parameters in an animal model of wound healing. *Lasers Med Sci* 26: 125–131.
41. Silveira, P.C.L., L.A. da Silva, C.A. Pinho, P.S. De Souza, M.M. Ronsani, D.L. Scheffer, *et al*. 2013. Effects of low-level laser therapy (GaAs) in an animal model of muscular damage induced by trauma. *Lasers Med Sci* 28: 431–436.
42. Vekshin, N.L., and G.P. Mironov. 1982. Flavin-dependent oxygen uptake in mitochondria under illumination. *Biofizika* 27: 537–539.
43. Karu, T. 1999. Primary and secondary mechanisms of action of visible to near-IR radiation on cells. *J Photochem Photobiol B Biol* 49: 1–17.
44. Javierre, E., F.J. Vermolen, C. Vuik, and S. Van der Zwaag. 2009. A mathematical analysis of physiological and morphological aspects of wound closure. *J Math Biol* 59: 605–630.
45. Chai, J., H. Song, Z. Sheng, B. Chen, H. Yang, and L. Li. 2003. Repair and reconstruction of massively damaged burn wounds. *Burns* 29: 726–732.
46. Khalil, B.K., Z. Khodr, and Z. Khalil. 2001. Modulation of inflammation by reactive oxygen species: implications for aging and tissue repair. *Free Radicals Biol Med* 30: 1–8.
47. Proksch, E., J.M. Brandner, and J.M. Jensen. 2008. The skin: an indispensable barrier. *Exp Dermatol* 17: 1063–1072.
48. Servetto, N., D. Cremonezzi, J.C. Simes, M. Moya, F. Soriano, J.A. Palma, *et al*. 2010. Evaluation of inflammatory biomarkers associated

with oxidative stress and histological assessment of low-level laser therapy in experimental myopathy. *Lasers Surg Med* 42: 577–583.
49. Gomes, L.E.A., E.M. Dalmarco, and E.S. Andre. 2012. The brain-derived neurotrophic factor, nerve growth factor, neurotrophin-3, and induced nitric oxide synthase expressions after low-level laser therapy in an axonotmesis experimental model. *Photomed Laser Surg* 30: 642–647.
50. Laraia, E.M.S., I.S. Silva, D.M. Pereira, F.A. dos Reis, R. Albertini, P. de Almeida, *et al*. 2012. Effect of low-level laser therapy (660 nm) on acute inflammation induced by tenotomy of Achilles tendon in rats. *Photochem Photobiol* 88: 1546–1550.
51. Wu, Q., W. Xuan, T. Ando, T. Xu, L. Huang, Y.Y. Huang, *et al*. 2012. Low-level laser therapy for closed-head traumatic brain injury in mice: effect of different wavelengths. *Lasers Surg Med* 44: 218–226.
52. Rizzi, C.F., J.L. Mauriz, D.S.F. Corrêa, A.J. Moreira, C.G. Zettler, L.I. Filippin, *et al*. 2006. Effects of low-level laser therapy (LPLT) on the nuclear factor (NF)-κB signaling pathway in traumatized muscle. *Lasers Surg Med* 38: 704–713.
53. Schauer, C., C. Janko, L.E. Munoz, Y. Zhao, D. Kienhöfer, B. Frey, *et al*. 2014. Aggregated neutrophil extracellular traps limit inflammation by degrading cytokines and chemokines. *Nat Med* 20: 511–7.
54. Lim, W., J.H. Kim, E. Gook, J. Kim, Y. Ko, I. Kim, *et al*. 2009. Inhibition of mitochondria-dependent apoptosis by 635-nm irradiation in sodium nitroprusside-treated SH-SY5Y cells. *Free Radic Biol Med* 47: 850–857.
55. Karu, T.I., L.V. Pyatibrat, and N.I. Afanasyeva. 2005. Cellular effects of low power laser therapy can be mediated by nitric oxide. *Lasers Surg Med* 36: 307–314.
56. Lim, W., J. Kim, C. Lim, S. Kim, S. Jeon, S. Karna, *et al*. 2012. Effect of 635 nm light-emitting diode irradiation on intracellular superoxide anion scavenging independent of the cellular enzymatic antioxidant system. *Photomed Laser Surg* 30: 451–459.
57. Lubart, R., R. Lavi, H. Friedmann, and S. Rochkind. 2006. Photochemistry and photobiology of light absorption by living cells. *Photomed Laser Surg* 24: 179–185.
58. Filippin, L.I., M.J. Cuevas, E. Lima, N.P. Marroni, J. Gonzalez-Gallego, and R.M. Xavier. 2011. The role of nitric oxide during healing of trauma to the skeletal muscle. *Inflamm Res* 60: 347–356.
59. da Silva, J.P., M.A. da Silva, A.P.F. Almeida, I.L. Junior, and A.P. Matos. 2010. Laser therapy in the tissue repair process: a literature review. *Photomed Laser Surg* 28: 17–21.
60. Juranek, I., and S. Bezek. 2005. Controversy of free radical hypothesis: reactive oxygen species-cause or consequence of tissue injury? *Gen Physiol Biophys* 24: 263–278.
61. Shukla, A., A.M. Rasik, and G.K. Patnaik. 1997. Depletion of reduced glutathione, ascorbic acid, vitamin E and antioxidant defence enzymes in a healing cutaneous wound. *Free Radic Res* 26: 93–101.
62. Gutteridge, J.M.C., and B. Halliwell. 2013. Antioxidants: molecules, medicines, and myths. *Biochem. Biophys Res Commun* 93: 561–564.
63. Pompella, A., A. Visvikis, A. Paolicchi, V. De Tata, and A.F. Casini. 2003. The changing faces of glutathione, a cellular protagonist. *Biochem Pharmacol* 66: 1499–1503.